PDLIM2 is a marker of adhesion and β-catenin activity in triple-negative breast cancer

Orla T. Cox[1], Shelley J. Edmunds[1], Katja Simon-Keller[2], Bo Li[3], Bruce Moran[3], Niamh E. Buckley[4], Milan Bustamante-Garrido[1], Nollaig Healy[1], Ciara H. O'Flanagan[1], William M. Gallagher[3], Richard D. Kennedy[5], René Bernards[6], Carlos Caldas[7], Suet-Feung Chin[7], Alexander Marx[2] and Rosemary O'Connor[1]*.

[1]Cell Biology Laboratory, School of Biochemistry and Cell Biology, University College Cork, Cork, Ireland, [2]Institute of Pathology, University Medical Centre Mannheim, Heidelberg University, Germany, [3]School of Biomolecular & Biomedical Science, Conway Institute, University College Dublin, Dublin, Ireland, [4]School of Pharmacy, Queens University Belfast, Belfast, Northern Ireland, [5]Centre for Cancer Research and Cell Biology, Queens University Belfast, Northern Ireland, [6]Division of Molecular Carcinogenesis and Cancer Genomics Netherlands, The Netherlands Cancer Institute, Amsterdam, The Netherlands, [7]Cancer Research UK Cambridge Research Institute, Li Ka Shing Centre, Cambridge, UK.

Running Title: *PDLIM2 enhances β-catenin activity in TNBC*

Keywords: PDLIM2, adhesion, growth factor signaling, beta-catenin, TNBC biomarker.
Abbreviations: TNBC; triple-negative breast cancer

*__Corresponding author:__ Rosemary O'Connor, Cell Biology Laboratory, School of Biochemistry and Cell Biology, University College Cork, Ireland. Phone: +353 21 490 1312. Email: r.oconnor@ucc.ie

This study was supported by the Irish Cancer Society Collaborative Cancer Research Centre BREAST-PREDICT CCRC13GAL, Science Foundation Ireland Principal Investigator awards 11/PI/11139 and 16IA4505, a European Union FP7 Marie Curie Industry-Academia Partnerships and Pathways (IAPP) Programme 251480 BiomarkerIGF, and RATHER (Rational Therapy for Breast Cancer), a Collaborative Project funded under the European Union 7th Framework Programme (grant agreement no. 258967).

Conflict of interest statement: The authors declare no potential conflicts of interest.
Abstract: 225 words, **Main text:** approx. 4852 words
Number of Figures: 7
Number of Supplementary Figures: 6,
Tables: 2,
Graphical Abstract: 1
Number of References: 47

Abstract:

The PDLIM2 protein regulates stability of transcription factors including NF-κB and STATs in epithelial and hemopoietic cells. PDLIM2 is strongly expressed in certain cancer cell lines that exhibit an Epithelial-to-Mesenchymal phenotype, and its suppression is sufficient to reverse this phenotype. PDLIM2 supports the epithelial polarity of non-transformed breast cells, suggesting distinct roles in tumor suppression and oncogenesis. To better understand its overall function, we investigated PDLIM2 expression and activity in breast cancer. PDLIM2 protein was present in 60% of tumors diagnosed as triple-negative breast cancer (TNBC), and only 20% of other breast cancer subtypes. High PDLIM2 expression in TNBC was positively correlated with adhesion signaling and β-catenin activity. Interestingly, PDLIM2 was restricted to the cytoplasm/membrane of TNBC cells and excluded from the nucleus. In breast cell lines, PDLIM2 retention in the cytoplasm was controlled by cell adhesion, and translocation to the nucleus was stimulated by IGF-1 or TGFβ. Cytoplasmic PDLIM2 was associated with active β-catenin and ectopic expression of PDLIM2 was sufficient to increase β-catenin levels and its transcriptional activity in reporter assays. Suppression of PDLIM2 inhibited tumor growth in vivo, whereas over-expression of PDLIM2 disrupted growth in 3D cultures. These results suggest that PDLIM2 may serve as a predictive biomarker for a large subset of TNBC whose phenotype depends on adhesion-regulated β-catenin activity and which may be amenable to therapies that target these pathways.

Statement of Significance: This study shows that PDLIM2 expression defines a subset of triple-negative breast cancer that may benefit from targeting the β-catenin and adhesion signaling pathways.

Introduction:

Triple-negative breast cancers (TNBCs) lack estrogen receptor, progesterone receptor (ER^-, PR^-), and amplification of human epidermal growth factor receptor 2 ($HER2^-$), and constitute 15-20% of all breast cancers. TNBC displays considerable genetic heterogeneity, a high risk for distant metastasis, is refractory to many therapies, and often has a poor prognosis [1-5]. Although many studies have helped define subtypes within TNBC, the underlying drivers of this cancer are still unclear, and there is an urgent need for better biomarkers and therapeutic targets [5-7].

Growth factor and adhesion signaling have been strongly implicated in TNBC [8-11]. Our studies on Insulin-like Growth Factor-1 (IGF-1) signaling in cancer led us to identify the PDLIM2 (Mystique) protein [12], as a feedback regulator of IGF-1 and adhesion signaling [12-14]. PDLIM2 is a member of the PDZ-LIM domain family encoded by a locus on chromosome 8p21 [12, 15, 16], a region that is associated with metastasis and often disrupted in cancer [17]. Located at the cytoskeleton and nucleus of epithelial cells and hemopoietic cells, PDLIM2 regulates the stability and activity of important transcription factors including STATs, NF-κB and IRFs [12, 18-21]. PDLIM2 can suppress cellular transformation [12, 13, 16], and it may be repressed by methylation in breast cell lines [22, 23]. PDLIM2 inactivation has also been reported in classical Hodgkin and anaplastic large cell lymphoma [24]. On the other hand, PDLIM2 is robustly expressed in breast and prostate cancer cells that exhibit a migratory phenotype [13, 16], and sustains a transcription programme for Epithelial to Mesenchymal Transition (EMT) [21]. In line with this, PDLIM2 expression has been linked to highly aggressive ovarian cancer [25], lymph node metastasis in low-grade breast cancers [26] and was identified as a moderate dependency gene in basal breast cancers [27]. It has also been linked to the growth of Neurofibromatosis 2 (NF2)-associated menginioma and schwannoma [28].

In the non-tumorigenic MCF10A breast epithelial cell line, PDLIM2 is required for maintaining cell polarization and 3D acinar formation [14], and PDLIM2 expression increases upon retinoic-acid induced differentiation of breast cancer cells [23]. However, although PDLIM2 expression has been linked with tumor suppression and with sustaining a migratory phenotype, it is still unclear what it contributes to the progression or phenotype of any subgroup of breast cancer. Here, we investigated this by assessing PDLIM2 expression in different cohorts of breast tumors and manipulating its expression in cell lines. We found that PDLIM2 is expressed in a subset of triple-negative breast cancers (TNBCs; 50-60%), and

in approximately 20% of other breast cancer subtypes. In triple-negative tumors and cell lines, cytoplasmic PDLIM2 promotes the accumulation of active β-catenin. Our study suggests that PDLIM2 mediates adhesion and growth factor signals derived from the tumor microenvironment to enhance β-catenin activation in a large proportion of TNBCs.

Materials and Methods

Cell Culture and Assays

Cell lines were purchased from ATCC, except CAL-51 (DSMZ) and authentication established by PCR-single-locus-technology (Eurofins Medigenomix, Forensik GmbH, Ebersberg, Germany), up to November 2018. MDA-MB-231-LUC2 cells were purchased for *in vivo* experiments (Caliper Life Sciences). All cells were tested monthly for mycoplasma by specific DNA staining and maintained as previously described [14, 29, 30], up to 6-8 weeks for use in experiments. Further details can be found in supplementary methods: Tables 1, 3.

For serum starvation and growth factor stimulation, cells were incubated in serum-free medium for 4hr prior to stimulation, or not, with 10ng/ml TGF-β1 or IGF-1. For non-adherent conditions, cells were trypsinized, centrifuged and washed prior to re-suspension in complete medium into 50ml tubes. Cells were incubated for 4 hours at 37^{o}C, with gentle rotation. Alternatively, cells were seeded on petri dishes coated with 100µl/cm^{2} of Polyhema (6mg/ml) (Sigma, Dublin, Ireland).

For wound healing assays, confluent monolayer cultures were wounded by scoring with a sterile pipette tip, and imaged at 0hr and 24hr post-wounding. Wound widths were measured as described in Supplementary Methods.

Colony formation was measured by assessing plating efficiency. MDA-MB-231-LUC2 cells were seeded at 5 x 10^{2} cells/well in 6 well plates, (minimum triplicates per clone). After 9-10 days, cells were stained with 0.01% crystal violet and colonies of more than 50 cells were counted.

For 3D on Top assays, cells were cultured on matrigel with matrigel-supplemented medium, as described by Kenny *et al* [31] and monitored over 4 days. Entire 3D cultures were extracted for western blot analysis of protein expression as described [31].

In vivo bioluminescence imaging of tumor spread

Two separate clones of MDA-MB-231-LUC2 cells stably expressing shRNA scramble control or shRNA targeting PDLIM2 (1 ×10^{6} cells), were injected into the tail vein of 4-5

week old female HsdOla:MF1-*Foxn1*^{nu} mice (Harlan, UK; n = 6-7 per group, randomized; 3 separate cohorts). The Bioluminescent signal (luminescence counts) per animal per cell clone and images were collected after 45-49 days by using the IVIS® Spectrum *in vivo* imaging system (PerkinElmer, Dublin, Ireland). These experiments were performed under licence to R. O'Connor from the Irish Department of Health and protocol approval by University College Cork Animal Experimentation Ethics Committee (#2012/008). Further details are in supplementary Methods.

Cell lysates, Subcellular fractionations, Western blotting and Densitometry

Total cell protein was extracted using RIPA buffer and subcellular fractionations were performed as described previously [20, 32]. Western blot analyses were performed using the Odyssey Image scanner system and protein expression levels were normalized to protein loading control by densitometry using Licor Image Studio software as previously described [14, 20, 21, 32].

Breast Cancer tissue sample collections and Immunohistochemistry

All tissues were stained using a PDLIM2 mouse monoclonal antibody (Abcam). Details of immunohistochemistry (IHC) staining procedures used for each sample collection are described in supplementary methods.

Northern Ireland Biobank (NIB) cohort: Breast Cancer Tissue Microarrays were generated from Formalin-fixed paraffin-embedded primary tumor blocks as previously described [33]. Each tumor was represented by three independent cores. Breast Cancer subtypes were determined from biomarker expression, and classified according to St Gallen International Expert Consensus [34] as: Luminal A (ER and/or PR positive, HER2 negative); Luminal B (ER and/or PR positive and HER2 negative (HER2-) or HER2 overexpressed/amplified (HER2+)); HER2 enriched (non-luminal, ER and PR negative and HER2 overexpressed/amplified); Basal-like/Triple negative (ER, PR and HER2 negative).

RATHER TNBC cohorts: Slides from the Netherlands Cancer Institute (NKI) and Cambridge University (CAM) contained tissue cores from individual patients within the cohorts [35], and we analyzed IHC staining of tumor samples from 128 TNBC patients. Further details on RATHER cohorts analyses are in supplementary Methods.

Heidelberg samples: Breast Cancer Tissue sections were prepared from TNBC biopsies at the University Medical Centre Mannheim as described previously [36]. Further details are in supplemental methods. Written informed consent and ethical approval was obtained at each Institution [33, 35, 36].

RNA extraction, quantitative PCR, DNA, shRNA and siRNA Transfections

RNA extraction, cDNA synthesis and quantitative PCRs were performed as previously described [21], with details and primer sequences in supplementary methods/ Table 2.

MDA-MB-231-LUC2 cells were transfected with pSUPER vectors encoding shRNAs targeting PDLIM2 (shPDLIM2) or control shRNA (shScramble), and BT549 cells with pcDNA3-HA-Empty Vector (EV) or HA-PDLIM2 using Lipofectamine 2000. Stable clones were generated by selection in G418 [12, 21]. HEK293T cells were transiently transfected with HA-EV or HA-PDLIM2 using Calcium Phosphate protocol [32]. HCC1806 were transiently transfected with siRNA negative control and 2 different siRNAs targeting PDLIM2 using oligofectamine [12]. Further details are in supplementary Methods.

β-catenin/Tcf transcriptional reporter activity

HEK293T cells grown on 96-well OptiPlate microplates (PerkinElmer) were transfected with the TOPflash plasmid, which contains three copies of the Tcf/Lef sites upstream of a thymidine kinase (TK) promoter and the *firefly luciferase* gene, and the FOPflash, which contains mutated copies of Tcf/Lef sites using Lipofectamine 2000. Cells were co-transfected with 0.2 μg of internal control reporter *Renilla reniformis* luciferase construct (pRL-TK; Promega) to normalize transfection efficiency, and luciferase activity was measured using a dual luciferase Assay System kit (Promega).

Immunofluorescence staining

Cells were fixed with 4% paraformaldehyde, probed with primary antibodies followed by Alexa 488- or Cy3-conjugated secondary antibodies and/or TRITC-phalloidin. Nuclei were visualized with Hoechst dye and imaged as described previously [12, 14], and in supplementary methods.

RATHER cohorts RPPA, gene expression and subtype survival analysis

RNA was purified, amplified, labeled and hybridized to the Agendia custom-designed whole genome microarrays (Agilent Technologies) and raw fluorescence intensities quantified, as previously described [35]. GEO accessions are GSE66647 (RPPA) and GSE68057 (RNA microarray expression). Further details of analyses of the RATHER cohorts are in Supplementary Methods.

Kaplan-Meier survival analysis was performed using the SPSS statistics software (IBM). Univariate analysis was performed using the Cox regression model to illustrate the relationship between PDLIM2 protein expression and breast cancer-specific survival (BCSS), recurrence-free survival (RFS) and distant recurrence-free survival (DRFS), respectively. Hazard ratios (HRs) and 95% confidence intervals (95% CIs) were evaluated for each survival outcome using the Cox regression model.

Statistical Analysis:

Graphs were prepared using GraphPad Prism. Data were analyzed for statistical significance using Fisher's exact test, one way ANOVA or Student's *t*-test as indicated in legends. A p-value of <0.05 was deemed significant and graded p-values are denoted as follows: *p≤0.05; **p≤0.005; ***p≤0.0005, unless otherwise noted.

Results

PDLIM2 expression is enriched in Triple Negative Breast Cancer

To gain insight into how PDLIM2 contributes to human breast cancer, we first assessed its expression in tissue microarrays (TMAs) using IHC scored as negative (0), low (1), moderate (2) or high (3). Images representing the relative intensities of these IHC staining scores are shown in Suppl. Fig. 1A. In a TMA representing 248 breast tumors (Northern Ireland Biobank; NIB), PDLIM2 was expressed in 25.8% of all tumors (Fig. 1A). By separating these tumors using the Gallen scores of tumor classification [34], it was clear that the majority of Luminal A (HER2-negative), Luminal B-HER2-negative or -positive and HER2-enriched tumors did not express PDLIM2 (Fig. 1B, C). However, within the basal/TNBC samples more than half (53%) of tumors expressed PDLIM2 (Fig. 1B, C). Interestingly, PDLIM2 expression in tumor-associated stroma or tumor-infiltrating leukocytes was evident in 30-40% of all non-TNBC types in the TMA, and again, expression was proportionately higher in TNBC (61.8%; Fig. 1D, E, Suppl. Fig. 1B,C). Overall, 70% of PDLIM2-positive tumors (all subtypes) had PDLIM2-positive stroma, while within PDLIM2-negative tumors, 50% of TNBC and 30% of non-TNBC had PDLIM2-positive stroma (Suppl. Fig. 1C). PDLIM2 staining in TNBC and non-TNBC TMAs are shown in Fig. 1F and Suppl. Fig. 1D respectively.

In summary, PDLIM2 is expressed in more than 50% of TNBC tumor cells and 60% have PDLIM2-positive stroma, while in other breast cancer subtypes, it is expressed in approximately 20% of tumors and 40% of stroma.

The PDLIM2 protein is widely expressed in TNBC

PDLIM2 association with TNBC was further tested in additional TNBC cohorts. These were from the RATHER consortium (www.ratherproject.com), which includes cohorts from the Netherlands Cancer Institute, (NKI, n=71) and the University of Cambridge, UK (Cam; n=57). We also tested a smaller cohort (n=15) from Heidelberg University. As can be seen in Figure 2A, PDLIM2 was expressed in 53% of TNBC from the NIB cohort (data from Fig.1), 72% of the NKI cohort, 47% of the CAM cohort and 70% of the Heidelberg cohort (Figs. 2A, B). The distribution of weighted IHC scores for PDLIM2 staining is shown in Suppl. Fig. 2A. Overall, PDLIM2 was expressed in 60% of TNBCs across the four cohorts (Fig. 2C), and was low or absent in neighboring normal tissue, as shown in Suppl. Figure 2B (Heidelberg cohort). Interestingly, PDLIM2 is present in immune cells (mostly lymphocytes) surrounding epithelial ducts in this normal tissue (Suppl. Fig. 2B).

We next asked whether PDLIM2 expression could be correlated with survival and/or clinicopathological features. No significant correlation was found with PDLIM2 expression and overall survival in TNBC patients from the NIB cohorts, and in the RATHER cohorts, PDLIM2 was not significantly correlated with outcome (breast cancer specific-, recurrence free-, or distant recurrence-free survival; Suppl. Fig. 2C). Similar trends were observed when data were segregated into weighted scores, and there was no significant association with histological grade, number of positive lymph nodes, or tumor size (Suppl. Fig. 2C).

To test whether PDLIM2 is associated with specific TNBC subtypes we applied the 80 gene signature from Burstein et al., [6] to the RATHER cohorts (Fig. 2D). The majority of tumors were classified as mesenchymal (MES), but there was no significant correlation of PDLIM2 with any subtype (Fig. 2E; Suppl. Fig. 3A and B). However, trends indicated higher PDLIM2 expression in the Basal-like Immune Activated (BLIA) and Suppressed (BLIS) subtypes (the latter of which is associated with poorest outcomes [6]), compared with MES or Luminal Androgen Receptor (LAR) subtypes (Suppl. Fig. 3B, C). Interestingly, in these analyses, we noted that *PDLIM2* mRNA levels were not strongly correlated with PDLIM2 protein expression (Suppl. Fig. 3D).

Taken together, the data demonstrate that PDLIM2 is expressed in approximately 60% of tumor cells derived from four cohorts of TNBC, but is not definitively linked to TNBC subtypes or clinical outcomes.

PDLIM2 is restricted to the cytoplasm in TNBC tumors.

Since PDLIM2 subcellular location has previously been associated with integrating adhesion signals with transcription factor stability/activity [12, 20, 21], we next analyzed its location in TNBC tissue. It was clear that PDLIM2 is predominantly expressed at the cytoplasm/membrane and excluded from the nucleus in tumor cells (Fig. 3A). By quantifying PDLIM2 staining at the cytoplasm/membrane or also in the nucleus (nuclear-only expression was not observed in tumor cells), it was evident that PDLIM2 was restricted to cytoplasmic/membranous areas (Fig. 3B, C). This is in contrast to high levels of nuclear PDLIM2 in stromal cells (Fig. 1F insets, Suppl. Fig. 2B and 3E).

To determine functional significance for cytoplasmic PDLIM2 in TNBC, we used available reverse phase protein array (RPPA) and RNA profiling data for the RATHER cohorts, and asked whether PDLIM2 expression was associated with signaling pathways, or with transcription factor activity. Included in these analyses were 63 proteins and 139 genes with known or anticipated links to PDLIM2 function [12, 14, 18, 20, 21], (Suppl. Tables I and II). The Wilcoxon Rank Sum test was used to determine significance. RPPA data showed that high levels of phospho-β-catenin (serine 675; active) were significantly correlated with PDLIM2-positive tumors (Fig. 3D, Suppl. Table I). Phospho-MET (Tyrosine 1349) and the adhesion-associated proteins fibronectin and FAK, were also high in PDLIM2-positive tumors. In contrast, mTOR and Ki67 were low in PDLIM2-positive tumors (Fig. 3D). Interestingly, although the expression levels of several genes previously shown to be regulated by PDLIM2 [21], were significantly different in PDLIM2- negative and -positive tumors, mRNA levels corresponding to the differentially expressed proteins within the RPPA data were not significantly different (Suppl. Table II and IIb).

Overall, these data demonstrate that PDLIM2 expression in TNBC is restricted to the cytoplasm and this positively correlates with β-catenin activity and adhesion signaling.

PDLIM2 protein expression in TNBC cell lines is associated with adhesion and β-catenin levels.

To further test PDLIM2 association with specific signaling pathways in TNBC, we interrogated RNAseq and RPPA datasets available for approximately 80 breast cell lines [30]. PDLIM2 is not represented in the RPPA analysis but is present in the RNAseq data. Given the observed lack of correlation between *PDLIM2* mRNA and protein expression in the tumor samples (Suppl. Fig. 3D), we first tested whether *PDLIM2* mRNA could be correlated with protein expression in cell lines, using eight TNBC cell lines from the Marcotte study [30], and the triple-negative, non tumorigenic breast cell line, MCF10A, (classifications in

Suppl. Fig. 4A). In agreement with observations in tissues, we found that a subset of breast cell lines expressed high levels of PDLIM2 protein, whereas others did not (Fig. 4A and B).

Analysis of the RNAseq dataset from the triple-negative (TN) cell lines [30] demonstrated that *PDLIM2* RNA levels do not significantly correlate with protein expression (Suppl. Fig. 4B). The *PDLIM2* gene encodes several RNA variants including *PDLIM2* RNA variants 1, 2 and 3 (NM_198042, NM_021630, NM_176871; also referred to as *Mystique* 1, 2, 3). We previously reported that PDLIM2 protein is encoded by *PDLIM2* variant 2 [12, 16], and in the 9 TN cell lines, levels of *PDLIM2* variant 2 mRNA correlated well with protein (Fig. 4 C), whereas variant 3 *mRNA* was generally inversely correlated with protein (Fig. 4 D). *PDLIM2* variant 1 was barely detectable. Thus, since RNAseq data may include all *PDLIM2* RNA transcripts, it cannot be used to infer PDLIM2 protein expression. Moreover, since *PDLIM2* mRNA levels did not correlate with differentially expressed proteins in the RATHER cohorts (Fig. 3, Suppl. Tables I and II, IIb), our analyses indicate that PDLIM2 mRNA expression profiles in cancer cohorts do not reflect protein expression or function. This disparity may also explain why total *PDLIM2* mRNA does not correlate strongly with clinical outcomes.

Using the nine TN breast cell lines, we next asked whether PDLIM2 protein correlates with adhesion signals and β-catenin, as was observed in the RPPA data (Fig. 3D). β1-integrin was tested as a marker of extracellular matrix (ECM) adhesion, and we previously reported that PDLIM2 is essential for feedback regulation of β1-integrin signals [14]. E-cadherin and β-catenin are markers of cell-cell adhesion. β1-integrin was observed to be generally higher in PDLIM2-positive than PDLIM2-negative breast cell lines (Fig. 4E, G, Suppl. Fig. 4C). Furthermore, E-cadherin and β-catenin were also expressed at higher levels in PDLIM2-positive than PDLIM2-negative cells (Fig. 4E-G), with the exception of MDA-MB-231 cells where E-cadherin is suppressed by methylation [37]. In addition, β-catenin phosphorylated on Serine 675 was higher in PDLIM2-positive TN cells (Fig. 4E). Furthermore, levels of phospho-EGFR and phospho-IGF-1R were high in PDLIM2-positive TN cells (Suppl. Fig. 4D, E), although there was no clear correlation between phospho-c-MET and PDLIM2 expression (Suppl. Fig. 4F).

Overall, we conclude that PDLIM2 expression is associated with high levels of cell adhesion markers, active growth factor receptors and β-catenin.

PDLIM2 shuttling from cytoplasm to nucleus is stimulated by adhesion and growth factors.

Although PDLIM2 is restricted to the cytoplasm of TN tumors (Figs. 1-3), it could be observed in the cytoplasm and nucleus of cultured cell lines by both immunofluorescence and sub-cellular fractionation, (Fig. 5 A, B, Suppl. Fig. 5A, B). These observations suggest that cell adhesion and growth factors promote PDLIM2 shuttling between the cytoplasm and nucleus, so we tested this further. We found that under non-adherent culture conditions, PDLIM2 accumulates in the nucleus (Suppl. Fig. 5B, C). De-adhesion of MCF10A cells for 24h was sufficient to reduce PDLIM2 in the cytoplasm and induce accumulation in the nucleus, even under serum-starved conditions (Fig. 5C, D, Suppl. Fig. 5B, C). Re-adhesion of cells for up to 24hr was sufficient to restore cytoplasmic PDLIM2 with a concomitant decrease in nuclear levels (Fig. 5C). Thus, cell adhesion is necessary and sufficient for nuclear exclusion of PDLIM2.

Serum starvation caused markedly decreased nuclear and increased cytoplasmic PDLIM2 (Fig. 5 E-H, Suppl. Fig. 5C). Stimulation of MCF10A with either TGF beta (Fig. 5 E, G, H) or IGF-1 (Fig. 5F, G) promoted translocation of PDLIM2 into the nucleus over time. Interestingly, the substantial retardation of cytoplasmic PDLIM2 protein mobility, which we previously confirmed as serine phosphorylation [20], was less evident in the nuclear fractions (arrows; Fig. 5E, F), indicating that PDLIM2 serine phosphorylation facilitates it cytoplasmic sequestration. Overall, these data show that adhesion and growth factor signaling in TN breast cells control PDLIM2 phosphorylation and sub-cellular localization.

PDLIM2 expression is sufficient to activate β-catenin in TNBC

Since PDLIM2 expression correlates with active β-catenin (Fig. 3D, Fig. 4E), we next asked whether PDLIM2 enhances β-catenin activity by using two approaches. First, we assessed active β-catenin in cell lines using an antibody that detects β-catenin only when it is not phosphorylated on serine 45 and therefore active [38]. This showed that PDLIM2-expressing cells generally express active β-catenin (Fig. 6 A). Exceptions were MDA-MB-231 cells, which express PDLIM2 in the presence of low β-catenin, and HS578T which do not express PDLIM2 but have high active β-catenin expression. Similar results were observed using the antibody that detects active β-catenin phosphorylated on serine 675 [38, 39] (Fig. 4E, Suppl Fig. 5D). Immunofluorescence staining illustrated that active β-catenin is present at the plasma membrane, throughout the cytoplasm and in the nucleus of PDLIM2-positive cells (Fig. 6B). Interestingly, in cells with low PDLIM2, active beta catenin is predominantly at the plasma membrane (Fig. 6B).

The second approach was to test the effects of ectopic HA-PDLIM2 expression on β-catenin activity. In BT549 cells, HA-PDLIM2 was mostly evident in the cytoplasm and at the actin cytoskeleton (Suppl. Fig. 5E). Higher total and active β-catenin levels (Fig. 6C, Suppl. Fig. 6A) were observed in the cytoplasm and nucleus (Suppl. Fig. 6A, B), and the migratory potential was enhanced compared to controls (Suppl. Fig. 6C). Furthermore, ectopic expression of PDLIM2 was sufficient to activate β-catenin in HEK293T cells in luciferase reporter assays (Fig. 6D, E). PDLIM2 suppression had minor effects on the levels of β-catenin and adhesion proteins, in HCC1806 cells and MDA-MB-231-LUC2 cells (Suppl. Fig. 6E, F).

Since active β-catenin is associated with PDLIM2 in TNBC tissues and cell lines (Fig. 3, Fig. 6A, B), and PDLIM2 is restricted to the cytoplasm of TNBC tumor cells (Fig. 3), we next asked whether the sub-cellular localization of PDLIM2 is important for β-catenin expression and activation. To test this, we used cell detachment to induce nuclear accumulation of PDLIM2 and serum starvation to induce nuclear exclusion, and then measured β-catenin levels and phosphorylation (activity) status in PDLIM2-positive and -negative cells. As expected, (Fig. 5, Suppl Fig. 5, [12, 20]), cells in suspension exhibited less cytoplasmic PDLIM2 than adherent cells, with a concomitant accumulation of nuclear PDLIM2 (Fig. 6F, Suppl. Fig. 6G, H). These cells showed a clear reduction in active β-catenin levels in both the cytoplasm and nucleus that was not evident in PDLIM2-negative cells. Serum starvation had little effect on levels of active β-catenin, indicating that nuclear PDLIM2 is not directly involved in regulating β-catenin levels or activity (Suppl. Fig. 6H, I). We also confirmed that over-expressed HA-PDLIM2 accumulated more in the nucleus than in the cytoplasm in non-adherent BT549 cells, and this was accompanied by a marked reduction in active β-catenin, especially in the nucleus (Fig. 6G).

Overall, we conclude that PDLIM2 accumulation in the cytoplasm (and out of the nucleus) enhances nuclear levels of active β-catenin.

PDLIM2 suppression impairs TNBC tumor spread *in vivo* and alters spheroid growth.

In a previous study PDLIM2, suppression in DU145 prostate cells was shown to reverse the EMT phenotype characterized by re-expression of epithelial markers and loss of directional migration [21]. In that study we also showed MDA-MB-231-LUC2 cells with stably suppressed PDLIM2 exhibited enhanced proliferative rates and reduced growth in soft agarose compared to controls. As can be seen in Figures 7A and B, two clones of MDA-MB-231-LUC2 cells stably expressing shRNA targeting PDLIM2 (shPDLIM2) exhibited greatly

reduced colony formation (plating efficiency) compared to controls (shScr). To test the *in vivo* significance of PDLIM2 suppression in TNBC, we assessed *in vivo* tumour spread of these MDA-MB-231-LUC2 clones in nude mice. Each of the shPDLIM2 clones exhibited little if any tumor burden after 45-49 days compared to controls, noting that control shScr 1 cells exhibited better growth *in vivo* than shScr 2 (Fig. 7C). This result is consistent with reduced clonogenic growth and migratory potential previously observed with PDLIM2 suppression [21], and suggests that high PDLIM2 may facilitate breast cancer progression.

To further test PDLIM2 function, we assessed the effects of PDLIM2 overexpression on BT549 3D cell growth using 3D 'on top' cell culture assays [31]. In control BT549 cultures, cells formed stellate 3D structures that have previously been associated with an invasive phenotype [31]. However, BT549 cells stably expressing HA-PDLIM2 with higher active β-catenin, initially formed more rounded, small clustered structures than controls at day 2, and failed to fully adopt the stellate morphology by day 4 (Fig. 7D, E). These results indicate that PDLIM2 regulates the pathway controlling the stellate phenotype and also indicates that β-catenin activity is regulated during this reversible process.

Discussion:

Although several studies have characterized distinct types of TNBC [1-3, 6, 7], there remains an urgent need for biomarkers with prognostic value or to predict TNBC subgroups that would be amenable to novel therapies. Here, we found that the PDLIM2 protein is enriched in triple-negative breast cancers (overall approximately 60%), while it is less frequently expressed in other breast cancers. Furthermore, the correlation of PDLIM2 expression with β-catenin activity and adhesion signaling suggests it defines a large cohort of TNBC with similar features. A direct link between PDLIM2 expression in TNBC and clinicopathological parameters was not established. However, this may be due to TNBC heterogeneity and the fact that PDLIM2 mRNA profiles in available TNBC databases actually represent several *PDLIM2* mRNA variants, while only one mRNA variant (2) encodes protein. Our conclusion that the PDLIM2 protein is a marker for a large subset of TNBC is further supported by published genomic studies, including a gene dependency screen, that identified PDLIM2 as a moderate dependency gene in basal TNBC and functionally linked this to cell adhesion [27]. Interestingly, this study also reported that basal TNBC is addicted to proteasomal activity, while genes encoding components of the proteasome and the COP9 signalosome (CSN) have been described as essential in TNBC basal A cell lines [30]. These observations are all

consistent with the reported actions of PDLIM2 in shuttling between the cytoskeleton and nucleus to regulate transcription factor stability [19, 21, 40], via association with the COP9 signalosome [21].

Suppression of PDLIM2 in MDA-MB-231 (and DU145) cells is sufficient to impair migratory potential and clonogenic growth [21], and as shown here, to impair *in vivo* spread of MDA-MB-231-LUC2 cells, while re-introduction of PDLIM2 into BT549 TNBC cells alters their invasive growth in 3D cultures and enhances directional migration. The exclusion of PDLIM2 from the nucleus of tumor cells, and the effects of adhesion and growth factors on promoting PDLIM2 translocation from the cytoplasm to nucleus in cell cultures, indicate that adhesion signaling promotes cytoplasmic retention of PDLIM2 in TNBC to regulate its function. Moreover, TN cell lines expressing cytoplasmic PDLIM2 generally also expressed high levels of β1-integrin, E-cadherin, β-catenin, and phosphorylated IGF-1 or EGF Receptors. However, although PDLIM2 suppression enhanced expression of integrins and ECM proteins in a MCF10A 3D model [14], suppression of PDLIM2 in TNBC cell lines did not have a significant effect on the levels of β1-integrin, for example. This may be expected considering the high levels of adhesion proteins in PDLIM2-expressing TNBC cells, and that PDLIM2 is itself regulated by, and a component of adhesion signaling in these cells. Overall, we propose that PDLIM2 functions to maintain a polarized phenotype associated with cell-cell adhesion in normal epithelial cells, but in cancer cells, it is a component of adhesion signaling that promotes loss of cell polarization, tumour growth, and motility.

Our findings indicate that β-catenin activity is a key output of cytoplasmic PDLIM2 in TNBC. Levels of active β-catenin were significantly elevated in PDLIM2-positive tumors and ectopic expression of PDLIM2 was sufficient to induce β-catenin expression and activity in cell lines. This is consistent with suppression of PDLIM2 in EMT-like cells causing reduced β-catenin nuclear activity [21]. Several studies have linked canonical and atypical WNT/β-catenin signaling to breast cancer, although the role of β-catenin is complex [41-44]. Canonical WNT signaling in TNBC may promote stabilization of β-catenin in the cytoplasm and subsequent transcription of genes involved in EMT [44]. However, elevated β-catenin at the plasma membrane has been linked with a good prognosis in TNBC [42], while low β-catenin at cell membranes in EGFR-positive TNBC has been associated with poor survival [45]. Low levels of E-cadherin at cell membranes may also correlate with elevated β-catenin activity and poor survival in TNBC [46].

How PDLIM2 integrates adhesion and growth factor signaling to enhance β-catenin phosphorylation and activation is not fully established. It is likely that PDLIM2 mediates cell

adhesion-dependent phosphorylation and relocation of β-catenin to facilitate its subsequent nuclear activity. This is supported by our observations that cell de-adhesion reduces cytoplasmic PDLIM2 levels and phosphorylation/nuclear accumulation of active β-catenin, and that ectopic expression of PDLIM2 enhances β-catenin phosphorylation on serine 675 and its nuclear accumulation. Importantly, we also observed that although active β-catenin is low in PDLIM2-negative cell lines, it was predominantly at the plasma membrane or cell-cell contacts, whereas, in PDLIM2-positive cells, it was localized in the cytoplasm and nucleus. This suggests that PDLIM2 is not implicated in basal β-catenin phosphorylation, but rather, it facilitates the release of β-catenin from the membrane, thereby enabling its stabilization, phosphorylation and subsequent activation. Interestingly, growth factor and adhesion signals have recently been reported to act through cellular kinases such as SRC and PAK to enhance β-catenin phosphorylation on serine 675, and its subsequent activation [39, 47].

In summary, PDLIM2 is a marker for a large subgroup of TNBC that is driven by adhesion, growth factor signals and β-catenin activity. The identification of a potential new protein marker to classify functional subsets of TNBCs across previously defined subtypes is an important development. While PDLIM2 *per se* may not have a prognostic role, it could be a predictive biomarker to stratify TNBC for therapies that target the signaling pathways regulated by PDLIM2 or that directly target active β-catenin.

Acknowledgements

This work was funded by the Irish Cancer Society Collaborative Cancer Centre Breast Predict CCRC13GAL (to WM. Gallagher, R. O'Connor, supported OT Cox, B. Li, B. Moran,), Science Foundation Ireland Principal Investigator awards 11/PI/1139 and 16/IA/4505 (to R. O'Connor, supported OT Cox, M Bustamente-Garrido), and the European Union FP7 Marie Curie Industry-Academia Partnerships and Pathways (IAPP) Programme 251480: BiomarkerIGF (to R. O'Connor, supported S E. Edmunds, OT. Cox, CH. O'Flannagan). The Northern Ireland Biobank (NIB) received funding from the HSC Research and Development Division of the Public Health Agency in Northern Ireland, Cancer Research UK through the Belfast CR- UK Centre, the Northern Ireland Experimental Cancer Medicine Centre, and the Friends of the Cancer Centre. The Northern Ireland Molecular Pathology Laboratory, which creates resources for the NIB has received funding from Cancer Research UK, the Friends of the Cancer Centre and the Sean Crummey Foundation. The Rational Therapy for Breast Cancer (RATHER), a Collaborative Project is funded under the European Union 7th Framework Programme (grant agreement no. 258967). We thank Dr.

Gary Loughran, University College Cork, for helpful discussions on *PDLIM2* RNA isoforms and RNAseq analysis.

References

1. Shah, SP, Roth A, Goya R, Oloumi A, Ha G, Zhao Y, *et al.* The clonal and mutational evolution spectrum of primary triple-negative breast cancers. Nature, 2012. 486(7403): p. 395-9.
2. Curtis, C, Shah SP, Chin SF, Turashvili G, Rueda OM, Dunning MJ, *et al.* The genomic and transcriptomic architecture of 2,000 breast tumours reveals novel subgroups. Nature, 2012. 486(7403): p. 346-52.
3. Liedtke, C, Bernemann C, Kiesel L , Rody A. Genomic profiling in triple-negative breast cancer. Breast Care (Basel), 2013. 8(6): p. 408-13.
4. Ali, HR, Rueda OM, Chin SF, Curtis C, Dunning MJ, Aparicio SA, *et al.* Genome-driven integrated classification of breast cancer validated in over 7,500 samples. Genome Biol, 2014. 15(8): p. 431.
5. Denkert, C, Liedtke C, Tutt A , von Minckwitz G. Molecular alterations in triple-negative breast cancer-the road to new treatment strategies. Lancet, 2016.
6. Burstein, MD, Tsimelzon A, Poage GM, Covington KR, Contreras A, Fuqua SA, *et al.* Comprehensive genomic analysis identifies novel subtypes and targets of triple-negative breast cancer. Clin Cancer Res, 2015. 21(7): p. 1688-98.
7. Lehmann, BD, Bauer JA, Chen X, Sanders ME, Chakravarthy AB, Shyr Y, *et al.* Identification of human triple-negative breast cancer subtypes and preclinical models for selection of targeted therapies. J Clin Invest, 2011. 121(7): p. 2750-67.
8. Bahhnassy, A, Mohanad M, Shaarawy S, Ismail MF, El-Bastawisy A, Ashmawy AM, *et al.* Transforming growth factor-beta, insulin-like growth factor I/insulin-like growth factor I receptor and vascular endothelial growth factor-A: prognostic and predictive markers in triple-negative and non-triple-negative breast cancer. Mol Med Rep, 2015. 12(1): p. 851-64.
9. Taliaferro-Smith, L, Oberlick E, Liu T, McGlothen T, Alcaide T, Tobin R, *et al.* FAK activation is required for IGF1R-mediated regulation of EMT, migration, and invasion in mesenchymal triple negative breast cancer cells. Oncotarget, 2015. 6(7): p. 4757-72.
10. Yin, HL, Wu CC, Lin CH, Chai CY, Hou MF, Chang SJ, *et al.* beta1 Integrin as a Prognostic and Predictive Marker in Triple-Negative Breast Cancer. Int J Mol Sci, 2016. 17(9).
11. Hamurcu, Z, Kahraman N, Ashour A , Ozpolat B. FOXM1 transcriptionally regulates expression of integrin beta1 in triple-negative breast cancer. Breast Cancer Res Treat, 2017.
12. Loughran, G, Healy NC, Kiely PA, Huigsloot M, Kedersha NL , O'Connor R. Mystique is a new insulin-like growth factor-I-regulated PDZ-LIM domain protein that promotes cell attachment and migration and suppresses Anchorage-independent growth. Mol Biol Cell, 2005. 16(4): p. 1811-22.
13. Cox, OT, O'Shea S, Tresse E, Bustamante-Garrido M, Kiran-Deevi R , O'Connor R. IGF-1 Receptor and Adhesion Signaling: An Important Axis in Determining Cancer Cell Phenotype and Therapy Resistance. Front Endocrinol (Lausanne), 2015. 6: p. 106.

14. Deevi, RK, Cox OT , O'Connor R. Essential function for PDLIM2 in cell polarization in three-dimensional cultures by feedback regulation of the beta1-integrin-RhoA signaling axis. Neoplasia, 2014. 16(5): p. 422-31.
15. Torrado, M, Senatorov VV, Trivedi R, Fariss RN , Tomarev SI. Pdlim2, a novel PDZ-LIM domain protein, interacts with alpha-actinins and filamin A. Invest Ophthalmol Vis Sci, 2004. 45(11): p. 3955-63.
16. Loughran, G, Huigsloot M, Kiely PA, Smith LM, Floyd S, Ayllon V, *et al.* Gene expression profiles in cells transformed by overexpression of the IGF-I receptor. Oncogene, 2005. 24(40): p. 6185-93.
17. Macartney-Coxson, DP, Hood KA, Shi HJ, Ward T, Wiles A, O'Connor R, *et al.* Metastatic susceptibility locus, an 8p hot-spot for tumour progression disrupted in colorectal liver metastases: 13 candidate genes examined at the DNA, mRNA and protein level. BMC Cancer, 2008. 8: p. 187.
18. Tanaka, T, Soriano MA , Grusby MJ. SLIM is a nuclear ubiquitin E3 ligase that negatively regulates STAT signaling. Immunity, 2005. 22(6): p. 729-36.
19. Tanaka, T, Grusby MJ , Kaisho T. PDLIM2-mediated termination of transcription factor NF-kappaB activation by intranuclear sequestration and degradation of the p65 subunit. Nat Immunol, 2007. 8(6): p. 584-91.
20. Healy, NC , O'Connor R. Sequestration of PDLIM2 in the cytoplasm of monocytic/macrophage cells is associated with adhesion and increased nuclear activity of NF-kappaB. J Leukoc Biol, 2009. 85(3): p. 481-90.
21. Bowe, RA, Cox OT, Ayllon V, Tresse E, Healy NC, Edmunds SJ, *et al.* PDLIM2 regulates transcription factor activity in epithelial-to-mesenchymal transition via the COP9 signalosome. Mol Biol Cell, 2014. 25(1): p. 184-95.
22. Qu, Z, Fu J, Yan P, Hu J, Cheng SY , Xiao G. Epigenetic repression of PDZ-LIM domain-containing protein 2: implications for the biology and treatment of breast cancer. J Biol Chem, 2010. 285(16): p. 11786-92.
23. Vanoirbeek, E, Eelen G, Verlinden L, Carmeliet G, Mathieu C, Bouillon R, *et al.* PDLIM2 expression is driven by vitamin D and is involved in the pro-adhesion, and anti-migration and -invasion activity of vitamin D. Oncogene, 2014. 33(15): p. 1904-11.
24. Wurster, KD, Hummel F, Richter J, Giefing M, Hartmann S, Hansmann ML, *et al.* Inactivation of the putative ubiquitin-E3 ligase PDLIM2 in classical Hodgkin and anaplastic large cell lymphoma. Leukemia, 2017. 31(3): p. 602-613.
25. Du, F, Li Y, Zhang W, Kale SP, McFerrin H, Davenport I, *et al.* Highly and moderately aggressive mouse ovarian cancer cell lines exhibit differential gene expression. Tumour Biol, 2016. 37(8): p. 11147-62.
26. Bouchal, P, Dvorakova M, Roumeliotis T, Bortlicek Z, Ihnatova I, Prochazkova I, *et al.* Combined Proteomics and Transcriptomics Identifies Carboxypeptidase B1 and Nuclear Factor kappaB (NF-kappaB) Associated Proteins as Putative Biomarkers of Metastasis in Low Grade Breast Cancer. Mol Cell Proteomics, 2015. 14(7): p. 1814-30.
27. Petrocca, F, Altschuler G, Tan SM, Mendillo ML, Yan H, Jerry DJ, *et al.* A genome-wide siRNA screen identifies proteasome addiction as a vulnerability of basal-like triple-negative breast cancer cells. Cancer Cell, 2013. 24(2): p. 182-96.
28. Bassiri, K, Ferluga S, Sharma V, Syed N, Adams CL, Lasonder E, *et al.* Global Proteome and Phospho-proteome Analysis of Merlin-deficient Meningioma and Schwannoma Identifies PDLIM2 as a Novel Therapeutic Target. EBioMedicine, 2017. 16: p. 76-86.

29. Neve, RM, Chin K, Fridlyand J, Yeh J, Baehner FL, Fevr T, *et al.* A collection of breast cancer cell lines for the study of functionally distinct cancer subtypes. Cancer Cell, 2006. 10(6): p. 515-27.
30. Marcotte, R, Sayad A, Brown KR, Sanchez-Garcia F, Reimand J, Haider M, *et al.* Functional Genomic Landscape of Human Breast Cancer Drivers, Vulnerabilities, and Resistance. Cell, 2016. 164(1-2): p. 293-309.
31. Kenny, PA, Lee GY, Myers CA, Neve RM, Semeiks JR, Spellman PT, *et al.* The morphologies of breast cancer cell lines in three-dimensional assays correlate with their profiles of gene expression. Mol Oncol, 2007. 1(1): p. 84-96.
32. Stanicka, J, Rieger L, O'Shea S, Cox O, Coleman M, O'Flanagan C, *et al.* FES-related tyrosine kinase activates the insulin-like growth factor-1 receptor at sites of cell adhesion. Oncogene, 2018.
33. Buckley, NE, Haddock P, De Matos Simoes R, Parkes E, Irwin G, Emmert-Streib F, *et al.* A BRCA1 deficient, NFkappaB driven immune signal predicts good outcome in triple negative breast cancer. Oncotarget, 2016. 7(15): p. 19884-96.
34. Goldhirsch, A, Wood WC, Coates AS, Gelber RD, Thurlimann B, Senn HJ, *et al.* Strategies for subtypes--dealing with the diversity of breast cancer: highlights of the St. Gallen International Expert Consensus on the Primary Therapy of Early Breast Cancer 2011. Ann Oncol, 2011. 22(8): p. 1736-47.
35. Michaut, M, Chin SF, Majewski I, Severson TM, Bismeijer T, de Koning L, *et al.* Integration of genomic, transcriptomic and proteomic data identifies two biologically distinct subtypes of invasive lobular breast cancer. Sci Rep, 2016. 6: p. 18517.
36. Riabov, V, Yin S, Song B, Avdic A, Schledzewski K, Ovsiy I, *et al.* Stabilin-1 is expressed in human breast cancer and supports tumor growth in mammary adenocarcinoma mouse model. Oncotarget, 2016. 7(21): p. 31097-110.
37. Graff, JR, Herman JG, Lapidus RG, Chopra H, Xu R, Jarrard DF, *et al.* E-cadherin expression is silenced by DNA hypermethylation in human breast and prostate carcinomas. Cancer Res, 1995. 55(22): p. 5195-9.
38. Taurin, S, Sandbo N, Qin Y, Browning D , Dulin NO. Phosphorylation of beta-catenin by cyclic AMP-dependent protein kinase. J Biol Chem, 2006. 281(15): p. 9971-6.
39. Zhu, G, Wang Y, Huang B, Liang J, Ding Y, Xu A, *et al.* A Rac1/PAK1 cascade controls beta-catenin activation in colon cancer cells. Oncogene, 2012. 31(8): p. 1001-12.
40. Yan, P, Fu J, Qu Z, Li S, Tanaka T, Grusby MJ, *et al.* PDLIM2 suppresses human T-cell leukemia virus type I Tax-mediated tumorigenesis by targeting Tax into the nuclear matrix for proteasomal degradation. Blood, 2009. 113(18): p. 4370-80.
41. Khramtsov, AI, Khramtsova GF, Tretiakova M, Huo D, Olopade OI , Goss KH. Wnt/beta-catenin pathway activation is enriched in basal-like breast cancers and predicts poor outcome. Am J Pathol, 2010. 176(6): p. 2911-20.
42. Geyer, FC, Lacroix-Triki M, Savage K, Arnedos M, Lambros MB, MacKay A, *et al.* beta-Catenin pathway activation in breast cancer is associated with triple-negative phenotype but not with CTNNB1 mutation. Mod Pathol, 2011. 24(2): p. 209-31.
43. Dey, N, Barwick BG, Moreno CS, Ordanic-Kodani M, Chen Z, Oprea-Ilies G, *et al.* Wnt signaling in triple negative breast cancer is associated with metastasis. BMC Cancer, 2013. 13: p. 537.
44. Pohl, SG, Brook N, Agostino M, Arfuso F, Kumar AP , Dharmarajan A. Wnt signaling in triple-negative breast cancer. Oncogenesis, 2017. 6(4): p. e310.
45. Lakis, S, Dimoudis S, Kotoula V, Alexopoulou Z, Kostopoulos I, Koletsa T, *et al.* Interaction Between Beta-Catenin and EGFR Expression by Immunohistochemistry

Identifies Prognostic Subgroups in Early High-risk Triple-negative Breast Cancer. Anticancer Res, 2016. 36(5): p. 2365-78.
46. Shen, T, Zhang K, Siegal GP , Wei S. Prognostic Value of E-Cadherin and beta-Catenin in Triple-Negative Breast Cancer. Am J Clin Pathol, 2016. 146(5): p. 603-610.
47. Gayrard, C, Bernaudin C, Dejardin T, Seiler C , Borghi N. Src- and confinement-dependent FAK activation causes E-cadherin relaxation and beta-catenin activity. J Cell Biol, 2018. 217(3): p. 1063-1077.

Figure Legends

Figure 1:

PDLIM2 expression is enriched in Triple Negative Breast Cancer

A: A Breast Cancer TMA of 248 samples from the Northern Ireland Biobank (NIB) was stained for PDLIM2 expression by immunohistochemistry. PDLIM2 expression was scored as negative (0), low (1), moderate (2) or high (3). Percentages of total negative or positive samples from the entire cohort are shown. **B, C:** The TMA samples were classified according to Breast Cancer subtype and percentage of PDLIM2 negative versus positive (B) and PDLIM2 expression scores within each tumor type was assessed (C). Sample numbers for each Breast cancer subtype are shown in brackets in B. **D, E:** The percentage of samples with PDLIM2 negative and positive expression in Tumor stroma/infiltrating cells was assessed and quantified across the cohort (D) and within each Breast Cancer subtype (E). **F:** Panels i-iv: Representative micrographs of PDLIM2 IHC staining in TNBCs showing tumor cell and stromal cell negative staining (i); Tumor positive/stroma negative (ii); Tumor negative/stroma positive (iii), and tumor positive/stroma positive (iv). Insets show higher magnification images demonstrating PDLIM2 staining in Tumor (T) or stroma (S) cells. ***P<0.0001, **P<0.005, *P<0.05, Fisher's exact test comparing PDLIM2 positive and negative tumors in TNBC versus each non-TNBC subtype; ### P<0.0001 denotes TNBC versus all non-TNBC subtypes in B, C and E. In C, only IHC score 1 tumors were statistically significant.

Figure 2:

PDLIM2 is expressed in a subset of TNBCs

A. PDLIM2 expression was examined and quantified in three cohorts of TNBC samples; RATHER Netherlands Cancer Institute (NKI) and Cambridge University (CAM) TMAs and Heidelberg tissues (Heidelberg). The graph represents the percentage of PDLIM2 positive and negative tumors within each of these three cohorts plus the NIB cohort from Fig. 1. The number of tumors in each cohort is shown in brackets. **B:** Representative micrograph images illustrating PDLIM2-negative and -positive tumor staining within each cohort showing negative (0), low (1) or moderate-high (2 or 3) staining intensities. Scale bars are 50µm (NIB, Heidelberg) or 25µm (NKI, CAM). **C:** Graph shows total PDLIM2-negative and -positive TNBCs across all four cohorts. p-value determined using the Student's *t*-test. **D:** The Heatmap depicts TNBC tumor subtypes from the RATHER NKI and CAM cohorts,

determined from an 80-gene signature according to Burstein *et al,* [6], as described in supplementary methods. **E:** Graph showing the percentage of PDLIM2-positive and -negative tumors within each TNBC subtype in the RATHER cohorts, determined from 80-gene signature as in D, NKI n=70, CAM n=45. In D, E: TNBC subtypes described by Burstein *et al,* [6] are denoted as: MES: Mesenchymal, BLIA: Basal-like Immune-Activated, BLIS: Basal-like ImmunoSuppressed, LAR: Luminal Androgen Receptor.

Figure 3:

PDLIM2 retention at the cytoplasm in TNBC and correlation with adhesion signaling.

A: Representative micrographs of a PDLIM2-positive tumor from each cohort examined, with higher magnification shown in lower panels to highlight PDLIM2 localization at the cytoplasm/membrane and lack of nuclear staining. **B:** PDLIM2 subcellular localization within the TNBC cells was scored for each PDLIM2-positive tumor, and scores are presented in graphs as percentage of positive PDLIM2-tumors for each cohort. (The RATHER-CAM samples were omitted from these analyses as diffuse staining in some samples confounded a distinct localization score). **C:** Overall localization of PDLIM2 is shown as the percentage of all PDLIM2-positive TNBCs across the three cohorts, n=99. Statistical significance was analyzed using a Student's *t*-test. **D:** Box and whiskers plots of RPPA data illustrating distribution and median of expression values of proteins differentially expressed in PDLIM2-negative (NEG) versus –positive (POS) tumors from the RATHER cohorts. Norm. RFU: normalized RPPA Fluorescence Units. Significant differences between negative and PDLIM2 expression intensity from immunohistochemical analysis are also shown (IHC score 1-3); Wilcoxon test (Rank Sum) *p value <0.05, **p <0.005.

Figure 4:

PDLIM2 expression in Triple Negative cell lines that also express adhesion receptors and β-catenin

A. Whole cell lysates were prepared from a panel of TN cell lines cultured for 48 hours in complete medium, and PDLIM2 expression was examined by Western blotting. Actin is loading control. The approximate protein molecular weights in kilodaltons (kDa) are indicated on the left of each western blot panel. **B.** PDLIM2 expression in each of the cell lines was quantified by densitometry and data are presented as fold difference in expression compared with MCF10A cells, set at 1. Mean expression ± SEM from five separate

experiments are shown. **C, D.** PDLIM2 mRNA expression was measured for *PDLIM2* variant 2 (C) and variant 3 (D) by qPCR. Primer details are listed in supplementary methods Table 2. Graphs represent mean ± SEM from at least 3 separate experiments. Statistical significance was analyzed using a Student's *t*-test, comparing mRNA expression in each cell line to MCF10A (*P=0.045 in C). **E-G:** TN breast cell lines were grown under normal conditions, lysed and examined for expression of adhesion signaling proteins β1-integrin, E-cadherin and β-catenin and phospho-ser675 β-catenin by western blotting. Data are representative of at least 3 experiments, protein expression was quantified by densitometry as described in methods (G), quantification of phospho-ser675 β-catenin is included in suppl Fig. 5D.

Figure 5:

Cytoplasmic and nuclear shuttling of PDLIM2 in response to adhesion and growth factor signals

A. Representative immunofluorescence micrographs from at least 3 separate experiments, showing PDLIM2 expression and localization in TN cell lines. The remainder of the cell panel is shown in Suppl. Figure 5A. Cells were co-stained with TRITC-Phalloidin (actin) and Hoechst (Nuclei). Scalebar is 20μm. **B:** Subcellular fractions were prepared from TN breast cells cultured for 48 hours in complete medium, and analyzed by western blotting for PDLIM2 expression. Fraction markers are Tubulin (Cytoplasm) and PARP (Nuclei); representative of at least three separate experiments. **C:** MCF10A were plated on polyhema-treated petri dishes to prevent adhesion for 24hr (suspension), followed by re-plating on tissue-culture treated plates to allow reattachment for 24 hr. PDLIM2 expression and localization was compared with adherent cells by subcellular fractionation and western blotting. A representative experiment of three is shown. **D:** Graph shows densitometric quantification of PDLIM2 expression in the cytoplasm or nuclei of adherent and suspension cells from 3 separate experiments. Graphs represent mean ± SEM, statistical significance was analyzed using Student's *t*-test. **E, F:** MCF10A cells were serum starved followed by stimulation with either 10ng/ml TGF beta (TGF-β1; E) or IGF-1 (F) for up to 24 hr. Cells were harvested at each time-point indicated, and processed for subcellular fractionation of cytoplasmic and nuclear fractions which were probed for PDLIM2, signaling pathway markers Phospho-Smad2 (TGF-β1) or Phospho-Akt serine 473 (IGF-1), and fraction markers vinculin (Cytoplasm) and PARP (Nuclear) by western blotting. Arrows indicate phosphorylated PDLIM2. **G:** Quantification of PDLIM2 expression and localization following serum starvation in presence or absence of Growth factor stimulation for 24 hr

(TGF-β1; left graph, IGF-1; right graph) from at least three separate experiments. Expression levels were measured by densitometry, graphs represent mean ± SEM and statistical significance was analyzed using Student's *t*-test. **H:** PDLIM2 expression and localization (grey/green) in MCF10A cells following serum starvation alone, or in presence of 10ng/ml TGF-β1. Representative images taken at 100X magnification of each condition from at least three separate experiments are shown. Co-staining with TRITC-Phalloidin (actin, red) and Hoechst (Nuclei, blue). Scale bars represent 20μm.*P≤0.05, **P≤0.005 in D, G.

Figure 6:

PDLIM2 expression is sufficient to activate β-catenin in TNBC

A: Immunoblots of whole cell lysates from TN breast cell lines grown under normal conditions for 48 hr, were probed with active β-catenin (non-phosphorylated serine 45), total β-catenin, PDLIM2 and tubulin antibodies. Graph shows quantification of active β-catenin expression, measured by densitometry, mean expression relative to that of MCF10A cells ± SEM is shown. Student's *t*-test analyses of significant differences in expression compared to those of MCF10A cells, which are set at 1; *P≤0.05, **p≤0.005, ***p≤0.0001. **B:** Immunofluorescence micrographs of TN breast cell lines grown on coverslips in complete medium for 24 hr. Cells were fixed and stained for antibodies against active β-catenin (phospho-Ser675; green) and PDLIM2 (red). Nuclei were stained with Hoechst (blue). Scale bars represent 20μm. **C, D:** BT549 cells (C) or HEK293T cells (D) were stably transfected with HA-Empty Vector (EV) or HA-PDLIM2 as described in Supplementary Methods. Cells were cultured under normal conditions for 48 hr and assessed for protein expression as in A. Graphs show quantification of active β-catenin expression (non-phospho-Ser 45), measured by densitometry, mean expression ± SEM, relative to that of HA-EV control cells. Data is from 3 separate stable clones of HA-EV and HA-PDLIM2- expressing cells. **p≤0.001, Student's *t*-test. **E:** HEK293T cells stably transfected with HA-Empty Vector (EV) or HA-PDLIM2 were assessed for β-catenin transcriptional activity using a β-catenin/TCF TOPflash luciferase assay as described in methods. Data from three separate experiments are presented as fold change ± SEM of transcriptional activity of HA-PDLIM2-expressing cells compared with HA-EV controls, ***p≤0.0001, Student's *t*-test. **F, G:** Subcellular fractions of adherent or suspension cells were prepared for PDLIM2-positive or negative TN cell lines (F) or BT549 stably expressing HA-EV or HA-PDLIM2 (G). Western blots of cytoplasmic and nuclear fractions were probed for active β-catenin (non-phospho-Ser 45; F, or phospho-Ser

675; G), β-catenin, PDLIM2, and fraction markers tubulin (Cytoplasm) and PARP (Nuclear), e: empty lane. Counterparts with additional cell lines for parts F and G are shown in Suppl. Figs. 6G, H.

Figure 7:

PDLIM2 suppression inhibits 3D and colony formation *in vitro* and growth of TNBC cells *in vivo*.

A: Western blot analyses of suppression of PDLIM2 expression in MDA-MB-231-LUC2 cells stably expressing shScramble (shScr) or shPDLIM2 (Clones 1, 2), used for in vivo studies. PDLIM2 expression was quantified by densitometry, normalized to shScr1 levels, n=5. ***p<0.0005, Student's *t*-test. **B:** Colony formation by MDA-MB-231-LUC2 clones was assessed by plating efficiency assay, n=3. **C:** Scatter Plot showing decreased tumor burden of tumor cells with PDLIM2 suppressed. Data are whole body bioluminescence counts 45-49 days post-tail vein injection, with two clones each of MDA-MB-231-LUC2 cells stably expressing shScr or shPDLIM2 (Clones 1, 2). Examples of IVIS images are also shown. The color scale depicts the photon flux (photons per second) emitted from animals. ***p<0.0005, **P<0.005; One way ANOVA, Bonferroni's post-test in B and C. **D:** Micrographs of 3D cultures formed by BT549 clones stably expressing HA-EV or HA-PDLIM2, taken on Day 2 and 4 following plating in a 3D 'on top' assay as described in materials and methods. Original magnification is 10x. **E:** 3D cultures extracted from Matrigel were lysed and analyzed by western blotting for expression of phospho-ser675 and total β-catenin, HA-PDLIM2 and Tubulin loading control.

Figure 1

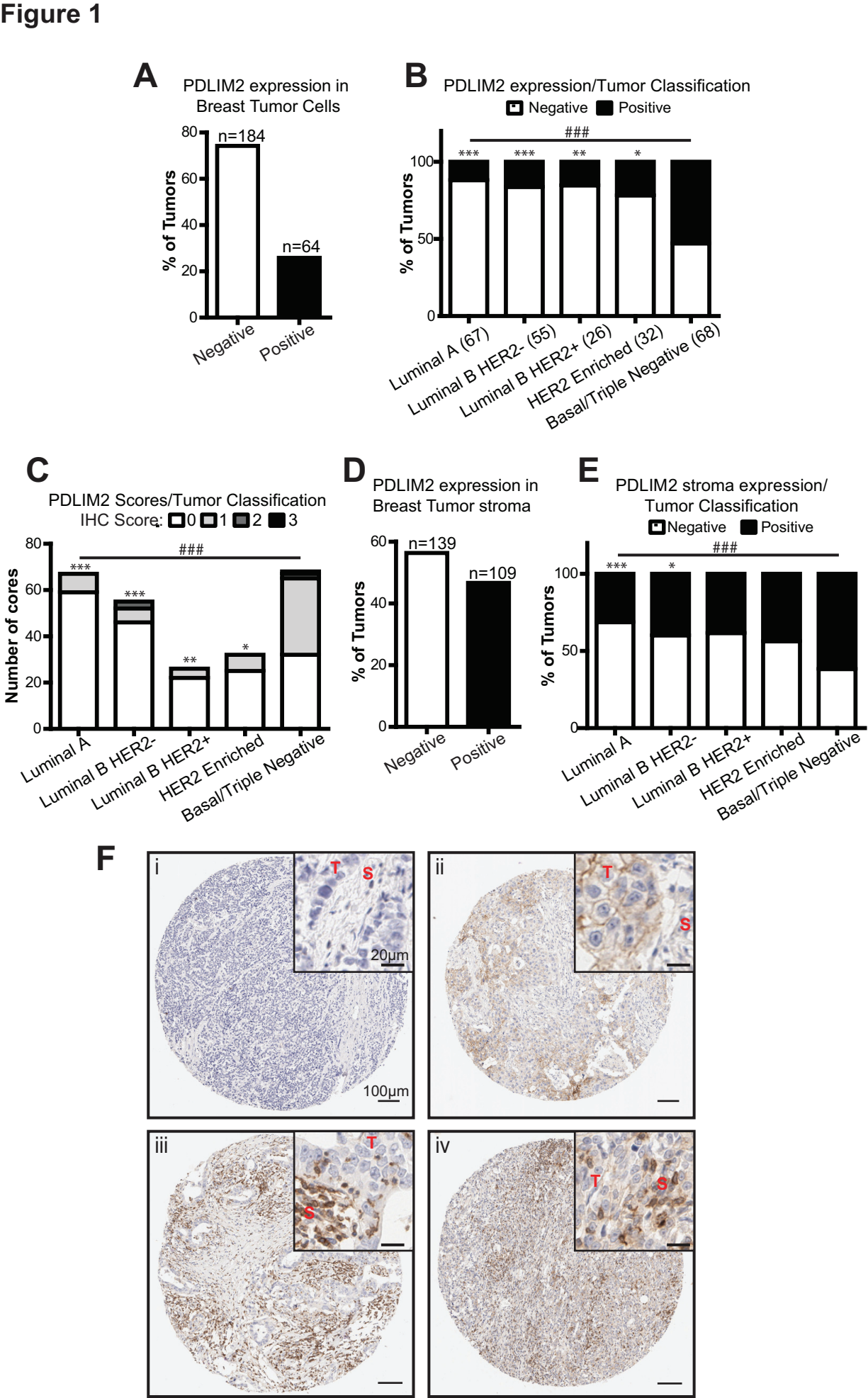
A
PDLIM2 expression in Breast Tumor Cells
% of Tumors
n=184
n=64
Negative
Positive
B
PDLIM2 expression/Tumor Classification
Negative
Positive
###
***
***
**
*
% of Tumors
Luminal A (67)
Luminal B HER2- (55)
Luminal B HER2+ (26)
HER2 Enriched (32)
Basal/Triple Negative (68)
C
PDLIM2 Scores/Tumor Classification
IHC Score: 0 1 2 3
Number of cores
###
***
***
**
*
Luminal A
Luminal B HER2-
Luminal B HER2+
HER2 Enriched
Basal/Triple Negative
D
PDLIM2 expression in Breast Tumor stroma
% of Tumors
n=139
n=109
Negative
Positive
E
PDLIM2 stroma expression/ Tumor Classification
Negative
Positive
###
***
*
% of Tumors
Luminal A
Luminal B HER2-
Luminal B HER2+
HER2 Enriched
Basal/Triple Negative
F
i
T
S
20μm
100μm
ii
T
S
iii
T
S
iv
T
S

Figure 2

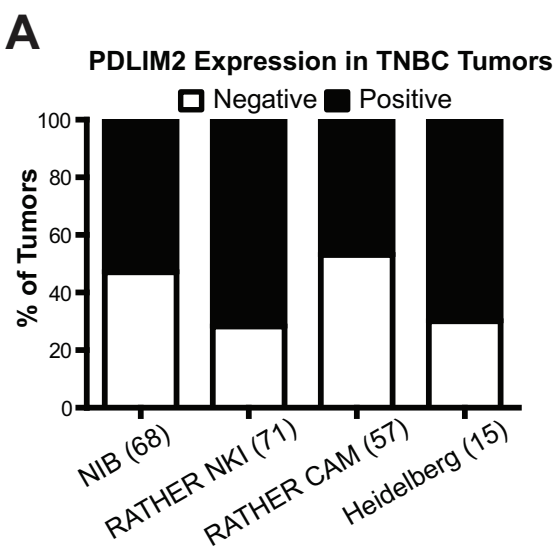
A
PDLIM2 Expression in TNBC Tumors
Negative
Positive
% of Tumors
100
80
60
40
20
0
NIB (68)
RATHER NKI (71)
RATHER CAM (57)
Heidelberg (15)

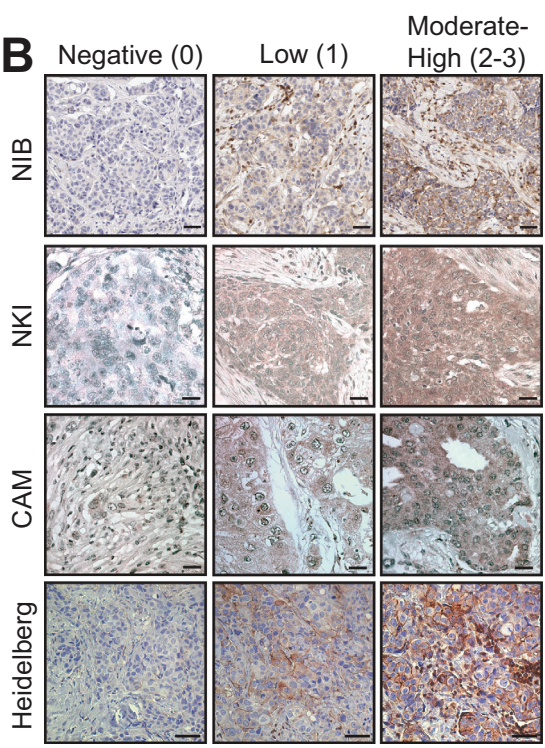
B
Negative (0)
Low (1)
Moderate-High (2-3)
NIB
NKI
CAM
Heidelberg

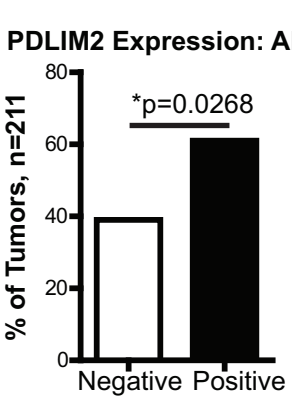
C
PDLIM2 Expression: All Cohorts
% of Tumors, n=211
*p=0.0268
80
60
40
20
0
Negative
Positive

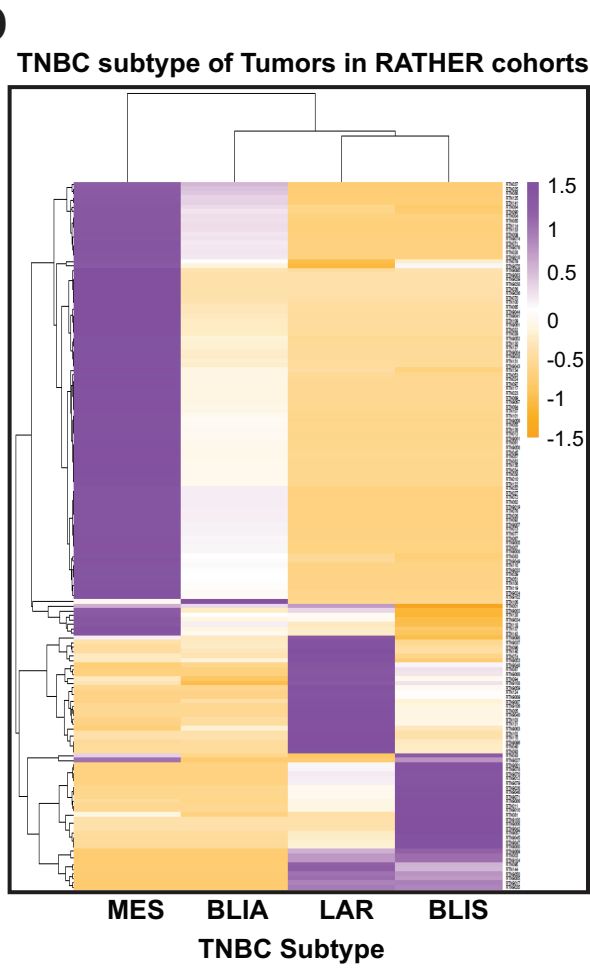
D
TNBC subtype of Tumors in RATHER cohorts
1.5
1
0.5
0
-0.5
-1
-1.5
MES
BLIA
LAR
BLIS
TNBC Subtype

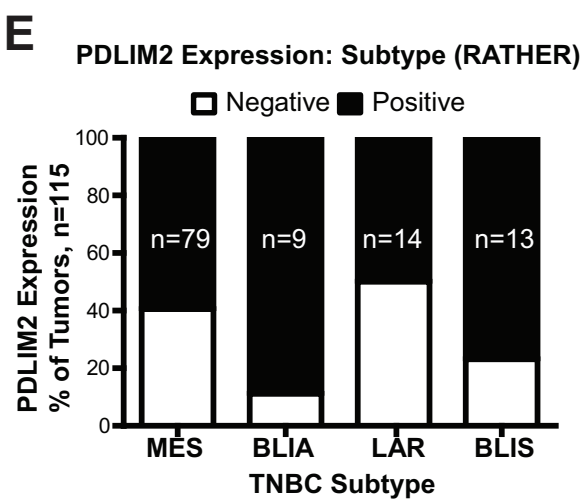
E
PDLIM2 Expression: Subtype (RATHER)
Negative
Positive
PDLIM2 Expression
% of Tumors, n=115
100
80
60
40
20
0
n=79
n=9
n=14
n=13
MES
BLIA
LAR
BLIS
TNBC Subtype

Figure 3:

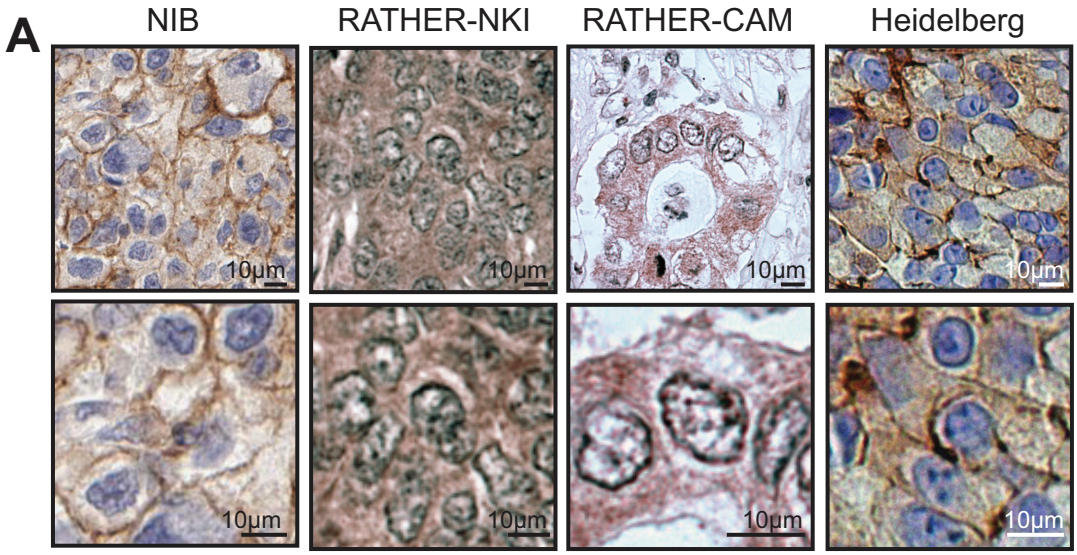

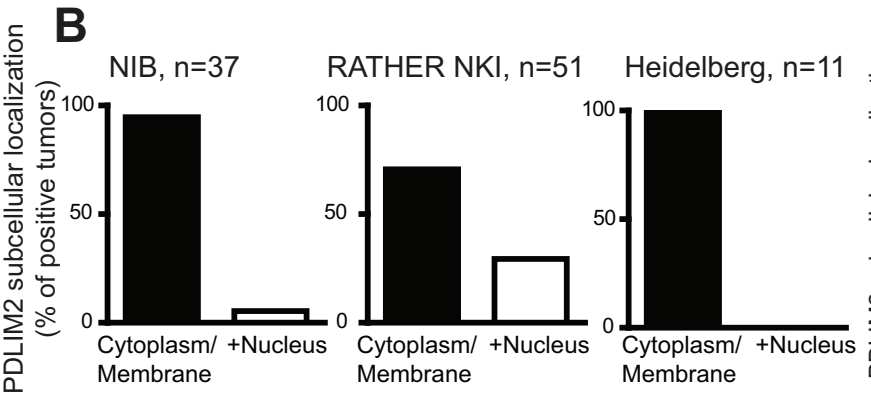

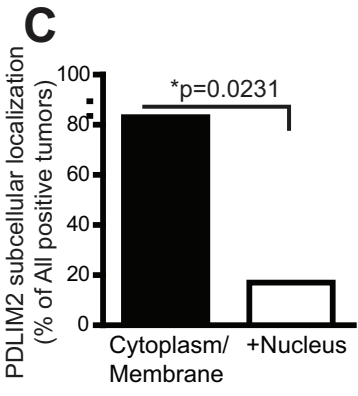

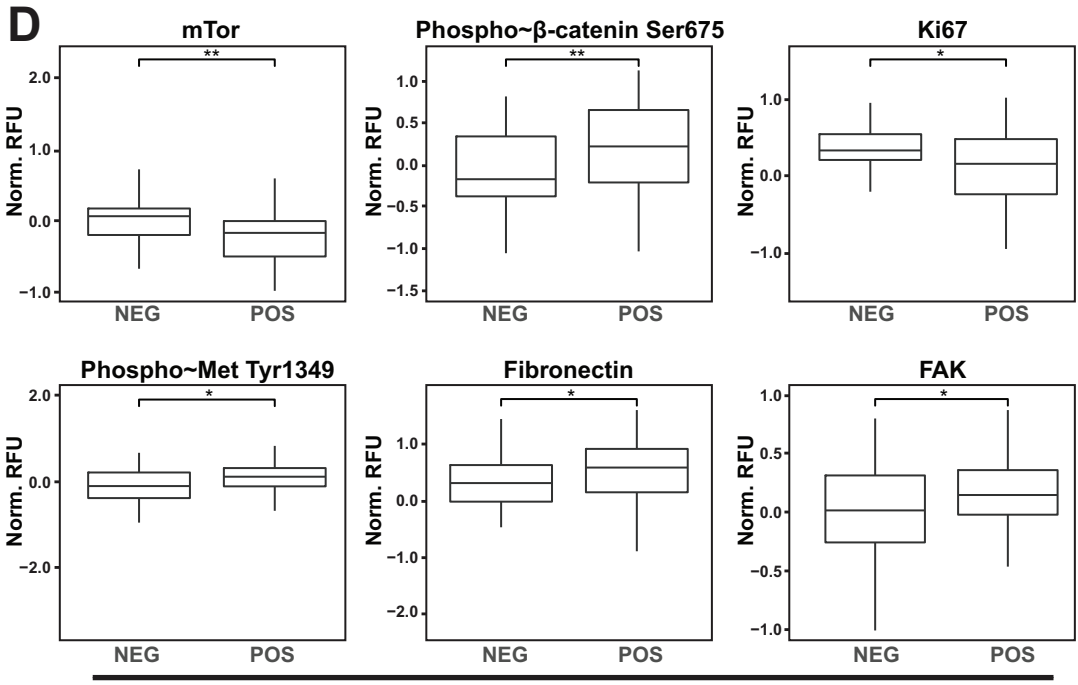

PROTEIN	Neg vs Pos	IHC Score 1	IHC Score 2	IHC Score 3
mTor	0.003**	0.065	0.012*	0.015*
Phospho-Beta Catenin Ser675	0.007**	0.254	0.024*	0.006**
Ki67	0.015*	0.064	0.009*	0.549
Phospho-Met Tyr1349	0.031*	0.480	0.030*	0.098
Fibronectin	0.040*	0.141	0.018*	0.806
Fak	0.043*	0.732	0.123	0.005**

Figure 4

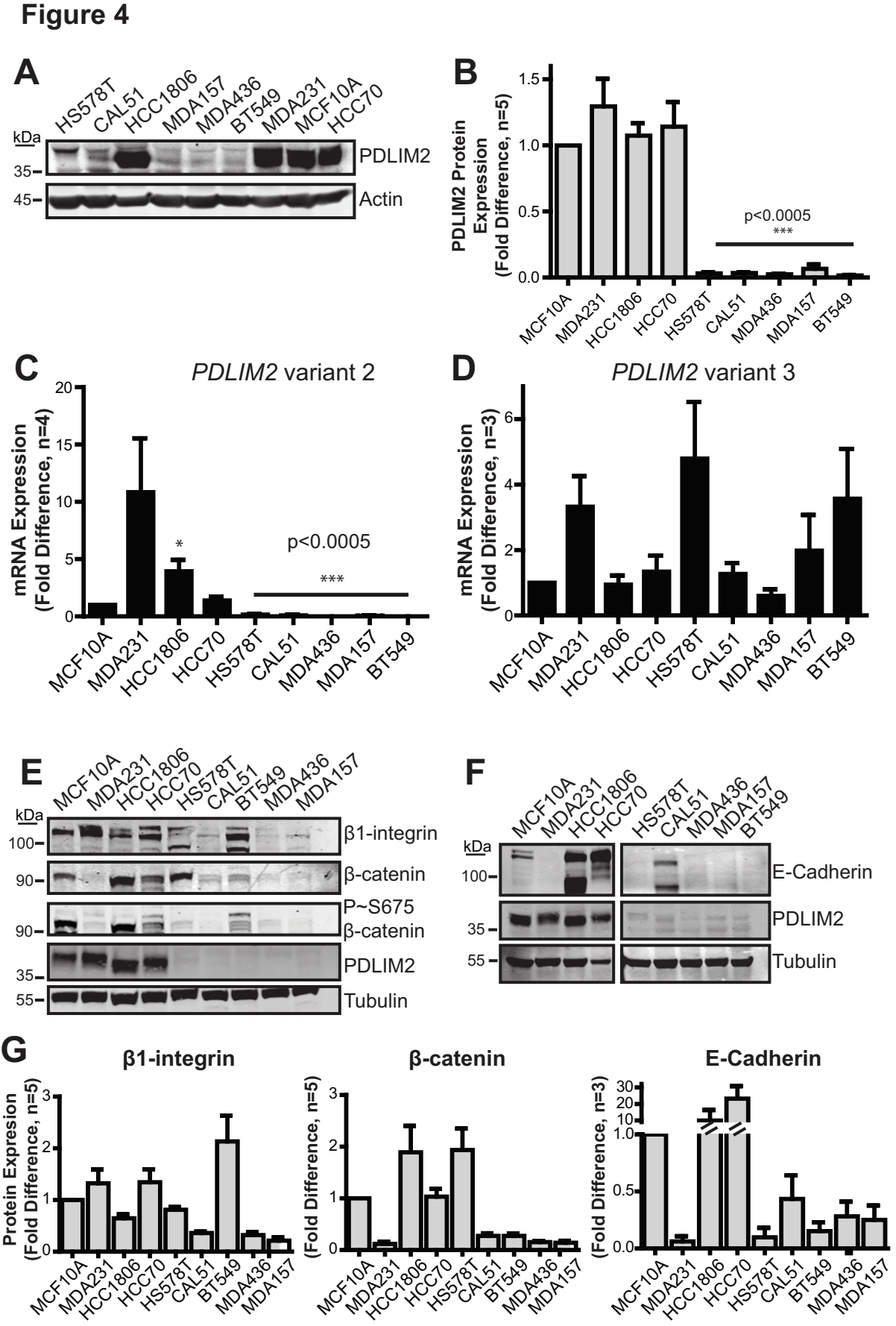
A
HS578T
CAL51
HCC1806
MDA157
MDA436
BT549
MDA231
MCF10A
HCC70
kDa
35
45
PDLIM2
Actin
B
PDLIM2 Protein Expression (Fold Difference, n=5)
1.5
1.0
0.5
0.0
p<0.0005
***
MCF10A
MDA231
HCC1806
HCC70
HS578T
CAL51
MDA436
MDA157
BT549
C
PDLIM2 variant 2
mRNA Expression (Fold Difference, n=4)
20
15
10
5
0
*
p<0.0005
***
MCF10A
MDA231
HCC1806
HCC70
HS578T
CAL51
MDA436
MDA157
BT549
D
PDLIM2 variant 3
mRNA Expression (Fold Difference, n=3)
6
4
2
0
MCF10A
MDA231
HCC1806
HCC70
HS578T
CAL51
MDA436
MDA157
BT549
E
MCF10A
MDA231
HCC1806
HCC70
HS578T
CAL51
BT549
MDA436
MDA157
kDa
100
90
90
35
55
β1-integrin
β-catenin
P~S675
β-catenin
PDLIM2
Tubulin
F
MCF10A
MDA231
HCC1806
HCC70
HS578T
CAL51
MDA436
MDA157
BT549
kDa
100
35
55
E-Cadherin
PDLIM2
Tubulin
G
β1-integrin
Protein Expresion (Fold Difference, n=5)
3
2
1
0
MCF10A
MDA231
HCC1806
HCC70
HS578T
CAL51
BT549
MDA436
MDA157
β-catenin
(Fold Difference, n=5)
3
2
1
0
MCF10A
MDA231
HCC1806
HCC70
HS578T
CAL51
BT549
MDA436
MDA157
E-Cadherin
(Fold Difference, n=3)
30
20
10
1.0
0.5
0.0
MCF10A
MDA231
HCC1806
HCC70
HS578T
CAL51
BT549
MDA436
MDA157

Figure 5:

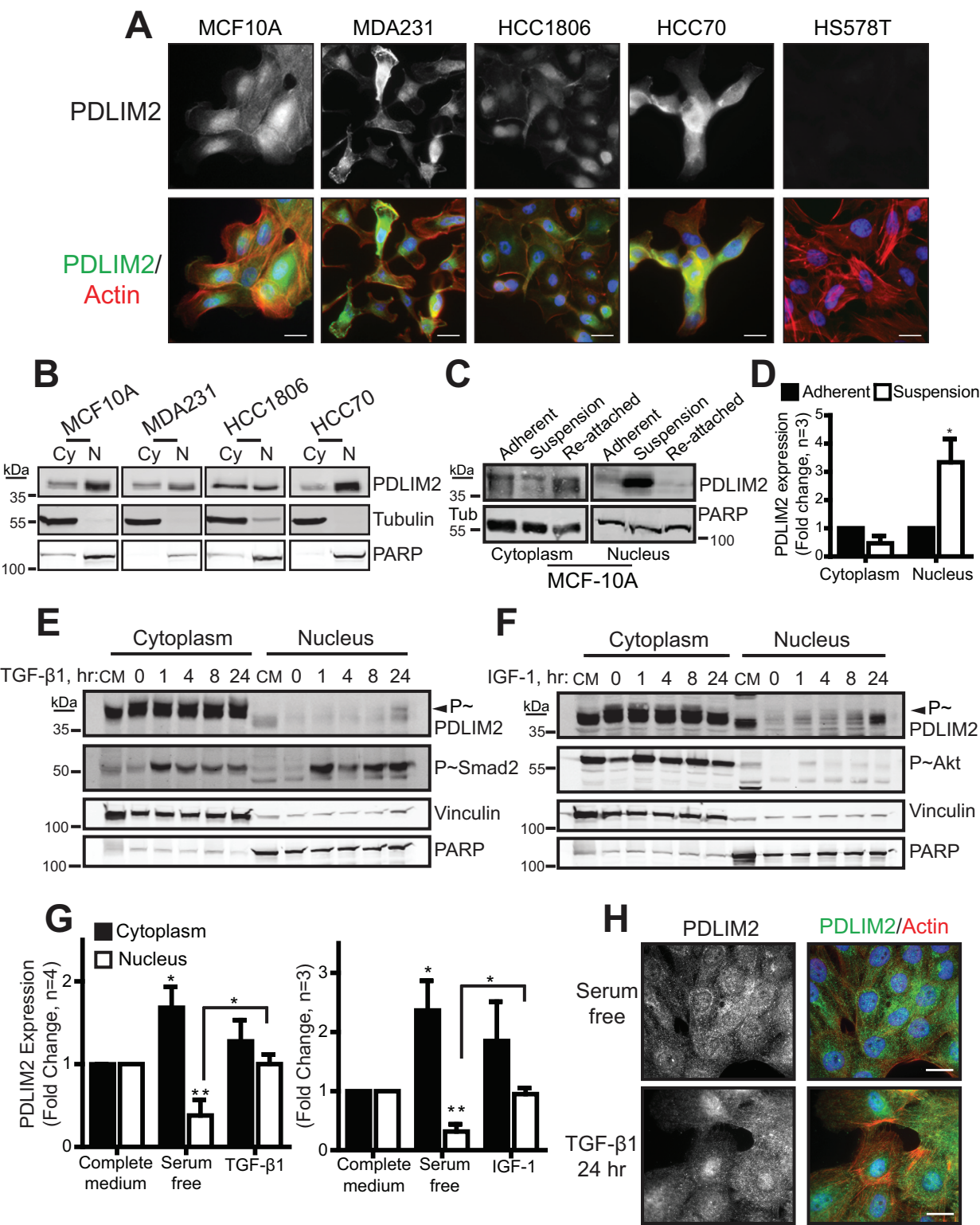
A
MCF10A
MDA231
HCC1806
HCC70
HS578T
PDLIM2
PDLIM2/
Actin
B
MCF10A
MDA231
HCC1806
HCC70
Cy N
kDa
35
55
100
PDLIM2
Tubulin
PARP
C
Adherent
Suspension
Re-attached
Adherent
Suspension
Re-attached
kDa
35
Tub
55
PDLIM2
PARP
100
Cytoplasm
Nucleus
MCF-10A
D
Adherent
Suspension
PDLIM2 expression
(Fold change, n=3)
5
4
3
2
1
0
*
Cytoplasm
Nucleus
E
Cytoplasm
Nucleus
TGF-β1, hr: CM 0 1 4 8 24 CM 0 1 4 8 24
kDa
35
50
100
100
◄P~
PDLIM2
P~Smad2
Vinculin
PARP
F
Cytoplasm
Nucleus
IGF-1, hr: CM 0 1 4 8 24 CM 0 1 4 8 24
kDa
35
55
100
100
◄P~
PDLIM2
P~Akt
Vinculin
PARP
G
Cytoplasm
Nucleus
PDLIM2 Expression
(Fold Change, n=4)
2
1
0
*
**
*
Complete
medium
Serum
free
TGF-β1
(Fold Change, n=3)
3
2
1
0
*
**
*
Complete
medium
Serum
free
IGF-1
H
PDLIM2
PDLIM2/Actin
Serum
free
TGF-β1
24 hr

Figure 6

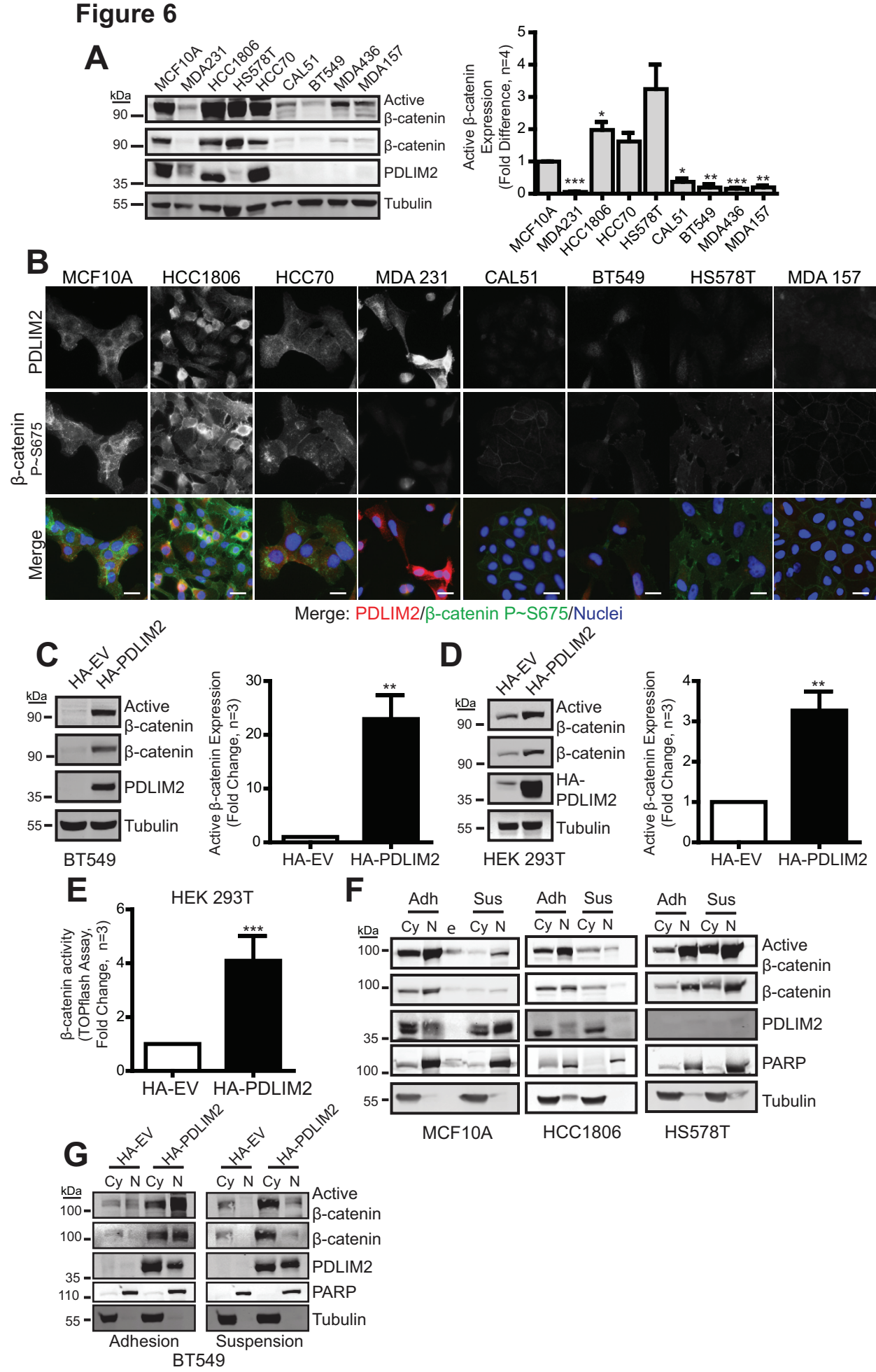
A
MCF10A
MDA231
HCC1806
HS578T
HCC70
CAL51
BT549
MDA436
MDA157
kDa
90
90
35
55
Active β-catenin
β-catenin
PDLIM2
Tubulin
Active β-catenin Expression (Fold Difference, n=4)
***
*
*
**
***
**
B
MCF10A
HCC1806
HCC70
MDA 231
CAL51
BT549
HS578T
MDA 157
PDLIM2
β-catenin P~S675
Merge
Merge: PDLIM2/β-catenin P~S675/Nuclei
C
HA-EV
HA-PDLIM2
Active β-catenin
β-catenin
PDLIM2
Tubulin
BT549
Active β-catenin Expression (Fold Change, n=3)
**
HA-EV
HA-PDLIM2
D
HA-EV
HA-PDLIM2
Active β-catenin
β-catenin
HA-PDLIM2
Tubulin
HEK 293T
Active β-catenin Expression (Fold Change, n=3)
**
HA-EV
HA-PDLIM2
E
HEK 293T
β-catenin activity (TOPflash Assay, Fold Change, n=3)
***
HA-EV
HA-PDLIM2
F
Adh
Sus
Cy N e Cy N
Active β-catenin
β-catenin
PDLIM2
PARP
Tubulin
MCF10A
HCC1806
HS578T
G
HA-EV
HA-PDLIM2
Cy N Cy N
Active β-catenin
β-catenin
PDLIM2
PARP
Tubulin
Adhesion
Suspension
BT549

Figure 7

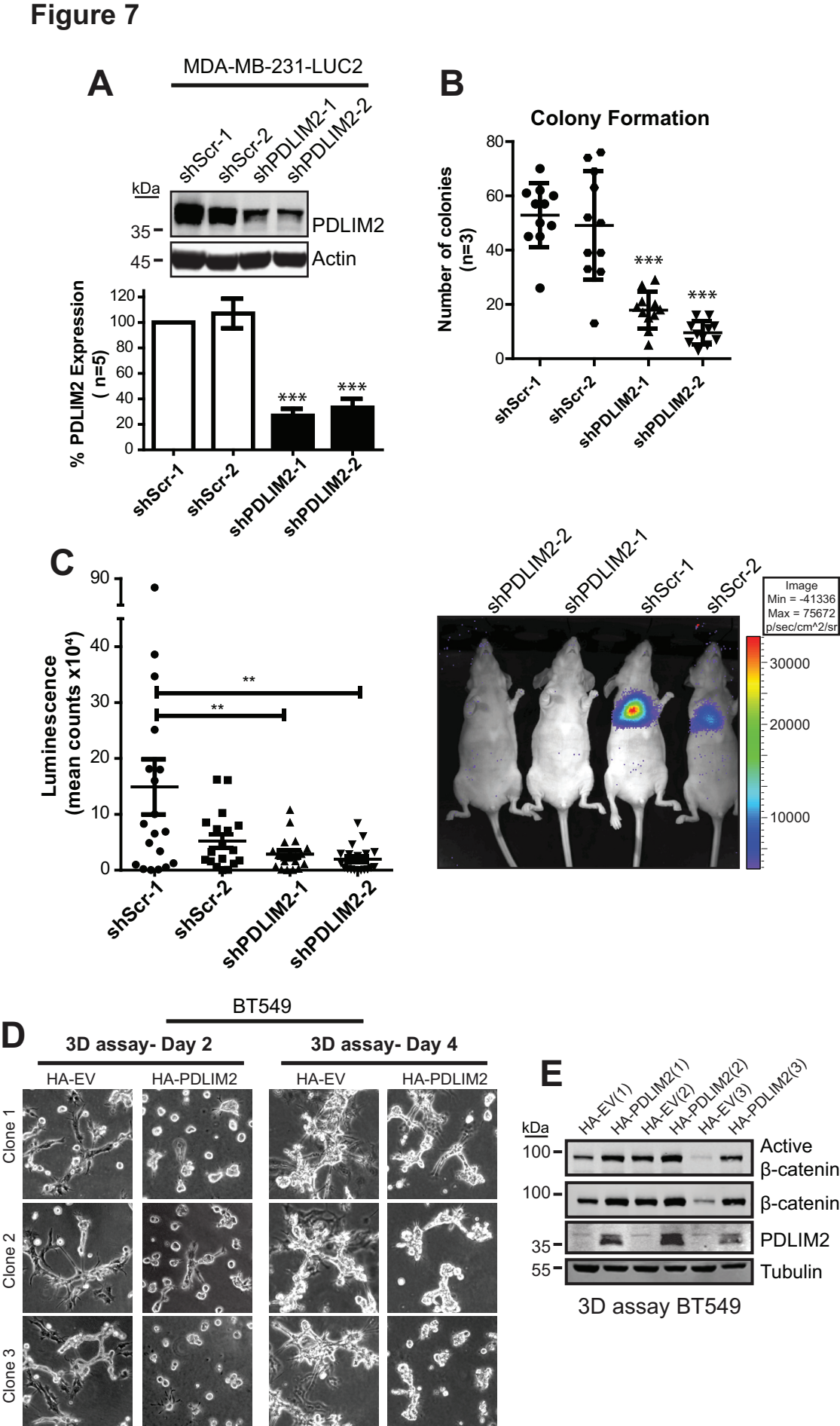
A
MDA-MB-231-LUC2
shScr-1
shScr-2
shPDLIM2-1
shPDLIM2-2
kDa
35
45
PDLIM2
Actin
% PDLIM2 Expression (n=5)
120
100
80
60
40
20
0
***
***
shScr-1
shScr-2
shPDLIM2-1
shPDLIM2-2
B
Colony Formation
Number of colonies (n=3)
80
60
40
20
0
***
***
shScr-1
shScr-2
shPDLIM2-1
shPDLIM2-2
C
Luminescence (mean counts x10⁴)
90
40
30
20
10
0
**
**
shScr-1
shScr-2
shPDLIM2-1
shPDLIM2-2
shPDLIM2-2
shPDLIM2-1
shScr-1
shScr-2
Image
Min = -41336
Max = 75672
p/sec/cm^2/sr
30000
20000
10000
BT549
D
3D assay- Day 2
3D assay- Day 4
HA-EV
HA-PDLIM2
HA-EV
HA-PDLIM2
Clone 1
Clone 2
Clone 3
E
HA-EV(1)
HA-PDLIM2(1)
HA-EV(2)
HA-PDLIM2(2)
HA-EV(3)
HA-PDLIM2(3)
kDa
100
100
35
55
Active β-catenin
β-catenin
PDLIM2
Tubulin
3D assay BT549